RSC Advances

PAPER

View Article Online
View Journal | View Issue

Cite this: *RSC Adv.*, 2022, **12**, 20857

Optimized preparation and performance evaluation of a bifunctional chitosan-modified flocculant†

Xiang Li, *[abc] Xianming Zhang,*[a] Shiyu Xie,[b] Yaling Ge,[d] Li Feng [e] and Wei Li[b]

Received 17th March 2022
Accepted 29th June 2022

DOI: 10.1039/d2ra01727j

rsc.li/rsc-advances

In view of the diversification of pollutants in current sewage, further improving the application efficiency of water treatment agents and realizing multi-functionalization are important directions for the research of water treatment agents. In this paper, on the basis of the natural polymer flocculant chitosan, MAPTAC and AM were used as modified monomers to improve its solubility and also enhance its flocculation and bactericidal properties. Furthermore, the preparation conditions of chitosan flocculant poly(CTS-*g*-AM-MAPTAC) were optimized by response surface methodology, and its flocculation and sterilization functions were evaluated in detail. The experimental results showed that the significance order of the factors in the preparation process was illumination time, mass ratio of total monomer to chitosan, molar ratio of monomers, and initiator concentration. The optimum conditions for preparing poly(CTS-*g*-AM-MAPTAC) were 6 moL L^{-1} for initiator concentration, 4 for mass ratio of total monomer to chitosan, 25% for monomer molar ratio, and 60 min for illumination time. The intrinsic viscosity and grafting rate of poly(CTS-*g*-AM-MAPTAC) prepared under optimum conditions were 5.4965 dL g^{-1} and 220.34%. The obtained poly(CTS-*g*-AM-MAPTAC) had good solubility, which could fully expose the active sites in wastewater with different acidity and had good flocculation effect. The performance evaluation results showed that the flocculant had a good combination of flocculation and sterilization, and had the advantages of high turbidity removal and sterilization efficiency, good biodegradability and low reagent consumption.

Introduction

One of the key points of municipal sewage treatment is the effective removal of pathogenic microorganisms, however the conventional disinfection treatment methods have the disadvantages of single treatment effect, secondary water pollution and limited application range. For example, some traditional water treatment processes include both flocculation and disinfection (sterilization). Such a water treatment process has the disadvantages that some residual organic flocculants in the flocculation treatment unit easily react with the oxidizing disinfection agent in the subsequent disinfection unit to produce substances toxic and harmful to human beings, aquatic animals and plants, and the bacterial sludge produced by the disinfection unit cannot be removed effectively.[1,2] Based on this, if a flocculant with both flocculation and disinfection effect can be developed, that is, the groups with both flocculation and bactericidal activity are spliced onto a polymer flocculant molecule by special chemical means, it will help to solve the above shortcomings of traditional water treatment process to some extent.

Studies have shown that the bactericidal functional group of some small molecule fungicides is the quaternary ammonium group,[3,4] and the quaternary ammonium group is a functional group that can enhance the electric neutralization of polymer flocculants.[5–8] Thus, quaternary ammonium groups are functional groups with bactericidal and flocculation activities. Theoretically, the amide cationic polyacrylamide (PAMA and TPAMA) prepared by authors in the early stage of the paper has the function of flocculation and sterilization.[9,10] However, the requirements of environmental protection for water treatment are becoming more and stricter, and the newly developed flocculants should have low or no toxicity. A certain amount of acrylamide monomer with neurotoxicity will be retained in the preparation process of acrylamide flocculant.[11–13] Therefore, acrylamide should be used less or avoided in the preparation of

[a]*Engineering Research Center for Waste Oil Recovery Technology and Equipment, Ministry of Education, Chongqing Technology and Business University, Chongqing 400067, China. E-mail: lx33cqu@163.com*

[b]*School of Civil Engineering and Architecture, Chongqing University of Science and Technology, Chongqing 401331, China*

[c]*Provincial and Ministerial Co-constructive of Collaborative Innovation Center for MSW Comprehensive Utilization, Chongqing University of Science and Technology, Chongqing 401331, China*

[d]*Key Laboratory of the Three Gorges Reservoir Regions Eco-Environment, State Ministry of Education, Chongqing University, Chongqing 400045, China*

[e]*School of Civil and Transportation Engineering, Guangdong University of Technology, No. 100, Waihuan Xi Road, Guangzhou Higher Education Mega Center, Panyu District, Guangzhou 510006, Guangdong, China*

† Electronic supplementary information (ESI) available. See https://doi.org/10.1039/d2ra01727j

organic flocculants for water treatment. Natural polymer chitosan (CTS) is recognized as a natural nontoxic polymer compound with certain flocculation and bactericidal effect, but it has the disadvantages of low water solubility and insufficient water treatment function.[14,15] Therefore, it is necessary to carry out corresponding chemical modification for its poor water solubility and low flocculation/sterilization function. Studies have been reported that the water solubility and bactericidal performance of CTS can be improved by introducing ionic groups and bactericidal group into molecules chain, respectively.[16,17] At present, most of the naturally modified CTS water treatment agents developed were aimed for enhancing one aspect of their function. There are still few studies on CTS water treatment agents with both efficient sterilization and flocculation function. In addition, the cationic flocculant prepared in previous study had the disadvantages of either low molecular weight affecting the bridging effect of flocculation process or low grafting rate of quaternary ammonium cation leading to weak electric neutralization. In order to make the prepared bifunctional flocculant have high viscosity and cationic grafting rate to improve the flocculation and bactericidal effect at the same time, it is necessary to optimize the preparation process.

In this paper, acrylamide (AM) and methyl acrylamide propyl trimethyl ammonium chloride (MAPTAC) with positive-charged quaternary ammonium group were selected as graft monomers. CTS was grafted and modified under UV irradiation. Finally, a flocculant poly(CTS-*g*-AM-MAPTAC) with high efficiency of flocculation and bactericidal properties was synthesized. The structure of poly(CTS-*g*-AM-MAPTAC) was analyzed by infrared spectroscopy (FTIR), X-ray diffraction (XRD), scanning electron microscopy (SEM) and differential thermogravimetric analysis (DSC-TG). The synthesis process was optimized by Box–Behnken experiment and response surface methodology (RSM). In addition, the flocculation and bactericidal properties of poly(CTS-*g*-AM-MAPTAC) were investigated in detail by kaolin suspension and simulated wastewater containing *Escherichia coli*.

Materials and methods

Materials

All the reagents used in the synthesis reaction were of analytical reagent grade except acrylamide (AM) and methacrylamido propyl trimethyl ammonium chloride (MAPTAC) (technical grade). The detail of reagents used in this study are as follows: AM (Chongqing Lanjie Tap Water Company, Chongqing, China); MAPTAC (50 wt% in water; Nanjing Jingruijiuan Biotechnology Co., Ltd Nanjing, China); VA-044 (Ruihong Biological Technology, Shanghai, China). CTS, acetic acid, absolute ethyl alcohol and other reagents were all purchased from Chongqing Chuandong Chemical Industry Co., Ltd Chongqing, China. *E. coli* original strain (CMCC 44102) was provided by the college of bioengineering, Chongqing University. All reagents were used in the experiment without further purification.

Preparation of poly(CTS-*g*-AM-MAPTAC)

CTS was pre-dissolved in 1% acetic acid solution. AM and MAPTAC with a certain mass ratio were then added to the chitosan acetic acid solution and continuously stirred into a homogeneous solution. After that, a certain quality of the initiator VA-044 was added after completely deoxygenated by bubbling with pure N_2 (99.99%). Then, the reaction vessel was immediately sealed and placed in the UV reactor for a predetermined time. The reaction products were aged for 2 hours and dried in a 50 °C vacuum oven to constant weight. The characterization methods of poly(CTS-*g*-AM-MAPTAC) was described in S1 text,† SEM and zeta potential analysis were described in S2 and S3 texts,† respectively.

Optimize synthesis conditions by RSM

The synthesis conditions of poly(CTS-*g*-AM-MAPTAC) were optimized by Box–Behnken (BBD) experiment and response surface methodology (RSM). In the experiment, initiator concentration (%) (A), mass ratio of total monomer to chitosan ($m_{(AM+MAPTAC)} : m_{CTS}$) (B), monomer molar ratio (%) ($n_{MAPTAC} : n_{(AM+MAPTAC)}$) (C) and illumination time (min) (D) were selected as the independent variables of BBD-RSM experiment, and grafting rate was used as the dependent variable. The detailed design of the BBD-RSM experiment is shown in Table 1. B_{29} (3^4) was used to improve the experiment. As given in Table 1 eqn (1) was used to account for the control and prediction of optimization process.

$$Y = \beta_0 + \sum_{i=1}^{k} \beta_i X_i + \sum_{i=1}^{k} \beta_{ii} X_i^2 + \sum_{i=1}^{k-1} \sum_{j=i+1}^{k} \beta_{ij} X_i X_j \qquad (1)$$

Performance evaluation experiment

100 mL of simulated wastewater was taken in 200 mL beaker, and the pH was adjusted with 0.1 M HCl or NaOH solution, then quantitative flocculant mother solution (1.0 g L^{-1}) was added and flocculation experiments were performed with a TA6 program-controlled coagulation experiment blender (200 rpm for 3 min, 40 rpm for 10 min, standing for 30 min). After flocculation, the supernatant was extracted by syringe at 1 cm below the liquid level for subsequent turbidity, zeta potential and OD_{600} determination. (All experiments were carried out three parallel samples, and the average value was taken as the final result.) The details of flocculants used in this part, preparation method of simulated wastewater and determination method of

Table 1 Experimental factors and levels of response surface design

		Level		
Factor	Code	−1	0	1
Initiator concentration (%)	A	5	6	7
$m_{(AM+MAPTAC)} : m_{CTS}$	B	3	4	5
$n_{MAPTAC} : n_{(AM+MAPTAC)}$	C	23	25	27
Illumination time (min)	D	45	60	75

water quality indexes were described in S4–S6 texts,† respectively.

Results and discussion

Structural characterization

FTIR spectra. In this paper, the synthesized products poly(CTS-*g*-AM-MAPTAC), PAMA (poly(AM-MAPTAC)) and CTS were scanned by infrared spectroscopy. The results are shown in Fig. 1(a)–(c).

As can be seen from Fig. 1(b), the peak at 2882 cm^{-1} corresponds to the asymmetric stretching vibration peaks of $-CH_3$ and $-CH_2$ in PAMA.[9] The peak at 1660 cm^{-1} represents –C=O stretching vibration peak; the peaks at 1495 and 1455 cm^{-1} represent the deformation vibration of quaternary ammonium methyl and methylene, respectively; the characteristic peak at 972 cm^{-1} represents the stretching vibration of $N^+-(CH_3)_3$.[18,19] The characteristic absorption peaks of CTS in Fig. 1(c) are O–H stretching at 3450 cm^{-1}, N–H deformation at 1640 and 1600 cm^{-1}, C–O–C stretching at 1160 cm^{-1}, and C–OH stretching at 1085 cm^{-1}.[19–21] Comparing the infrared spectra of poly(CTS-*g*-AM-MAPTAC) in Fig. 1(a) and CTS in Fig. 1(c), the absorption spectra of poly(CTS-*g*-AM-MAPTAC) and CTS are basically similar, indicating the basic skeleton of CTS was not affected in the process of graft copolymerization. At the same time, the stretching vibration peaks of –C=O, $N^+-(CH_3)_3$, $-CH_3$, $-CH_2$ and the deformation vibration peaks of quaternary ammonium methyl and methylene are also visible in the infrared spectra of poly(CTS-*g*-AM-MAPTAC), indicating that PAMA was successfully grafted into the CTS skeleton. It is confirmed that poly(CTS-*g*-AM-MAPTAC) was successfully prepared.

X-ray diffraction. The typical crystal structure characteristic absorption peaks of chitosan was observed at $2\theta = 14.0°$ and $2\theta = 20.8°$.[22,23] After grafting, the crystal structure changed to some extent, and the original characteristic absorption peak moved to about $2\theta = 24.0°$, and the intensity of the absorption peak was also relatively reduced. It is indicated that the introduction of AM and MAPTAC reduced the crystallinity of chitosan, which is mainly due to the introduction of side chains to increase the steric hindrance of CTS, thus weakening the hydrogen bond on the main chain of CTS, thereby damaging its crystal structure and making it amorphous. The XRD spectra also proved that AM and MAPTAC were successfully grafted onto the main chain of CTS (Fig. 2).

TG/DSC analysis. As shown in Fig. 3, CTS and poly(CTS-*g*-AM-MAPTAC) appeared two and three weight loss processes, respectively. In the first stage, the weight loss of the two was between 50 °C and 250 °C. The TG curves of CTS and poly(CTS-*g*-AM-MAPTAC) showed an obvious endothermic peak at 78.4 °C and 81.0 °C, respectively. This part of weight loss was mainly due to the decomposition of oligomeric chitosan and water evaporation.[24,25] But the small difference between the two was due to: (1) the introduction of quaternary ammonium groups in MAPTAC weaken the partial hydrogen bond and destroyed the complete crystal structure of chitosan. Therefore, –OH on CTS molecules was easy to contact with external water for hydration, increasing water evaporation of poly(CTS-*g*-AM-MAPTAC) at this temperature range. (2) The quaternary ammonium group is a hydrophilic group, which would increase the interaction force with water molecules, so higher temperature was needed to get rid of the water. The second stage of CTS weight loss was between 250 °C and 515 °C, and then the weight decreased gently. This part of the weight loss was mainly due to the degradation of the molecular main chain. However, the second weight loss temperature range of poly(CTS-*g*-AM-MAPTAC) was 250–360 °C, the weight loss rate was 26.1%, and the endothermic peak appeared at 300.2 °C. The weightlessness of this stage stemmed from the thermal decomposition and elimination reaction of the amide (–CONH–) in AM molecules, and the thermal separation of quaternary ammonium methyl and hydrogen chloride in the MAPTAC molecular chain.[24] The third weight loss was due to a broken C–C bond in the molecular backbone, resulting in a large decrease in the molecular weight.

In summary, the thermal stability of poly(CTS-*g*-AM-MAPTAC) was better than that of CTS. At the same time, the

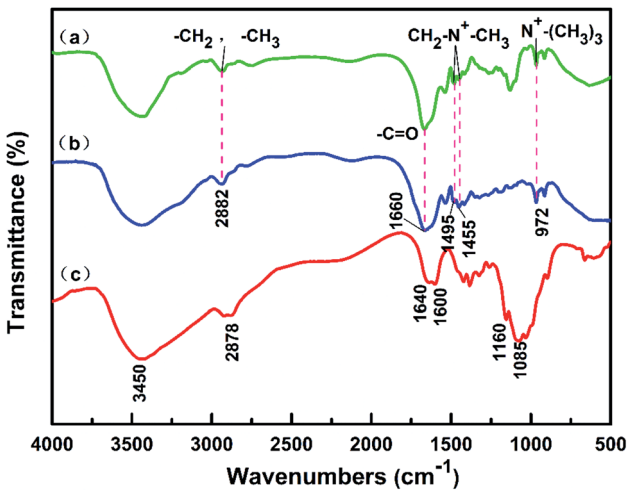

Fig. 1 The FT-IR spectra of (a) poly(CTS-*g*-AM-MAPTAC), (b) PAMA and (c) CTS.

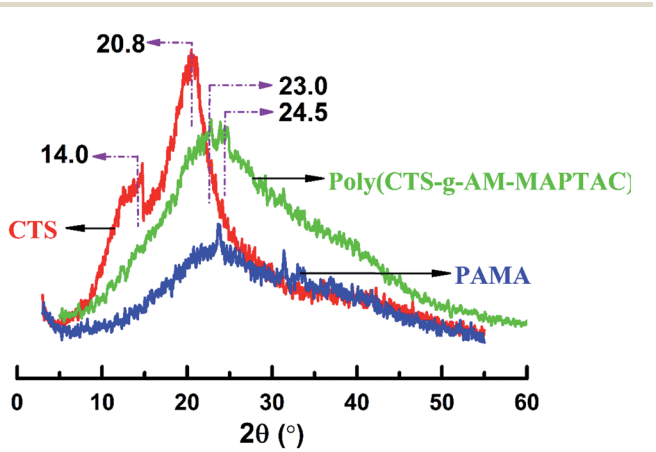

Fig. 2 X-ray diffraction diagrams of poly(CTS-*g*-AM-MAPTAC), PAMA and CTS.

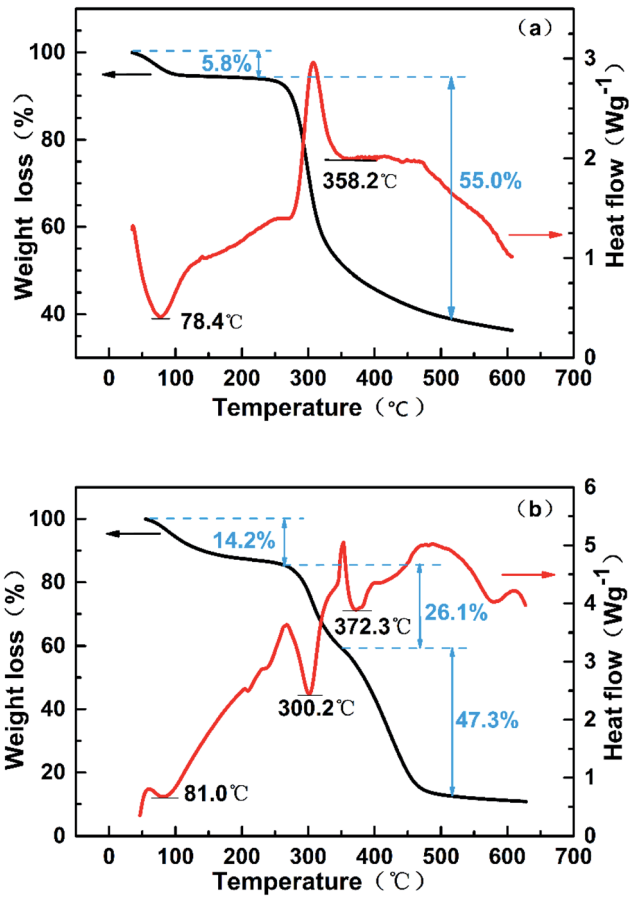

Fig. 3 TG/DSC graphs of (a) CTS and (b) poly(CTS-*g*-AM-MAPTAC).

inconsistency of DSC/TG curves indicated that there was a certain difference in structure between the two samples, which also proved that AM and MAPTACA were successfully grafted onto CTS.

BBD-RSM optimized synthesis conditions

Model establishment and variance analysis

Based on the optimization conditions determined by single factor, the response surface experiment scheme was designed using Box–Behnken model. Since the influence of product grafting rate on flocculation and sterilization performance was mainly considered in the subsequent application process, the grafting rate was selected as the response value in response surface design, and the interaction between initiator concentration (A), mass ratio of total monomer to chitosan (B), monomer molar ratio (C) and illumination time (D) was investigated. The combination of experimental conditions and the grafting rate of synthetic products under various conditions are shown in S7 text.†

The experimental results were analyzed by Design-Expert 8.0, and the linear regression equation between grafting rate and four factors was obtained as follows:

$$\text{Grafting ratio} = 222.52 - 1.50A + 1.90B + 1.63C + 4.01D - 0.80AB - 1.45AC - 2.30AD + 1.23BC - 2.33BD - 1.20CD - 12.24A^2 - 35.89B^2 - 17.07C^2 - 16.40D^2 \quad (2)$$

Further analysis of variance was performed to test the accuracy of the regression model. The results are shown in Table 2.

Generally, a larger F value or a smaller P value indicates that the corresponding factors have a good significance.[26,27] Table 2 shows the $F = 70.69$, $p < 0.0001$ of the regression model, indicating that the relationship obtained by this regression model between the grafting rate and the 4 factors was relatively accurate. The graft ratio predicted by eqn (2) was also close to the actual value. In addition, the missing items of the model were not obvious, indicating that some selected feature points could fit the whole situation well. Through the p value of the four factors, it can be judged that the significant order affecting the grafting rate of the product were D > B > C > A. Furthermore, the interactions between D and B, D and A, C and A were relatively obvious. Furthermore, the statistical analysis of the model errors are shown in S8 text.†

Response surface analysis

In order to study the influence of the interaction between different influencing factors on the grafting rate, the design expert software was used to make the three-dimensional response surface and contour map of the interaction of various factors according to the model. The results are shown in Fig. 4.

In Fig. 4(1)–(6), the interaction effects of AB, AC, AD, BC, BD and CD on grafting ratio are corresponding in turn. The greater the slope of the curve in the contour, the more obvious the influence of this factor. Also the deeper the color, the more significant the factor.[28–30] In Fig. 4(1), the three-dimensional response surface plots showed that with the increase of initiator concentration and the mass ratio of total monomer to chitosan, the grafting rate increased first and then decreased. The contour map showed that the optimum range of initiator concentration was 5.5–6.4 mol L^{-1}, and the mass ratio of total monomer to chitosan was 3.8–4.3. At the same time, the interaction of initiator concentration and mass ratio of total monomer to chitosan was not very obvious, and the effect of the latter on the grafting rate was more obvious. The remaining Fig. 4(2)–(6) were analyzed using the same analysis method. Through the overall comparative analysis, it can be seen that the combination of factors with obvious interaction were the mass ratio of total monomer to chitosan and illumination time, initiator concentration and illumination time. This result is consistent with Table 2 above.

Model verification

Based on the three-dimensional response surface diagram and contour map analysis, the predicted grafting rate of 222.89% would be achieved when the initiator concentration, the mass ratio of total monomer to chitosan, the monomer molar ratio and the illumination time were 5.92 mol L^{-1}, 4.02, 25.10% and

Table 2 ANOVA results of regression model

Source	Sum of squares	d*f*	Mean square	*F* value	*P* value prob > *F*	Significant
Model	9915.16	14	708.23	70.69	<0.0001	Significant
A	27.00	1	27.00	2.69	0.1229	
B	43.32	1	43.32	4.32	0.0564	
C	31.69	1	31.69	3.16	0.0971	
D	192.80	1	192.80	19.24	0.0006	
AB	2.56	1	2.56	0.26	0.6211	
AC	21.16	1	8.41	0.84	0.3751	
AD	8.41	1	21.16	2.11	0.1682	
BC	6.00	1	6.00	0.60	0.4518	
BD	21.62	1	21.62	2.16	0.1639	
CD	5.76	1	5.76	0.57	0.4609	
A^2	971.00	1	971.00	96.91	< 0.0001	
B^2	8352.86	1	8352.86	833.67	< 0.0001	
C^2	1890.62	1	1890.62	188.69	< 0.0001	
D^2	1744.07	1	1744.07	174.07	< 0.0001	
Residual	140.27	14	10.02			
Lack of fit	108.28	10	10.83	1.35	0.4133	Insignificant
Pure error	31.99	4	8.00			
Cor total	10 055.43	28				

61.85 min, respectively. Three additional independent experiments were carried out under the optimum condition. The average grafting rate was 220.34%, and the relative error with the predicted value of the model was 1.14%. It can be seen that the predicted value calculated by the regression equation was close to the actual value. The model could well reflect the influence of the synthesis conditions on the grafting rate of poly(CTS-*g*-AM-MAPTAC), and provided a strong basis for the preparation of products with better grafting rate.

Performance evaluation

Turbidity removal of kaolin suspension. Because kaolin is a negatively charged double electric layer aluminum silicate, its zeta potential is negative throughout the entire pH range (Fig. S3-2†).[31–33] Theoretically, cationic flocculant is more suitable for turbidity removal of kaolin suspension.[34,35] In this section, the effect of flocculant dosage, wastewater pH and grafting rate of poly(CTS-*g*-AM-MAPTAC) on the flocculation effect were investigated and the flocculation application

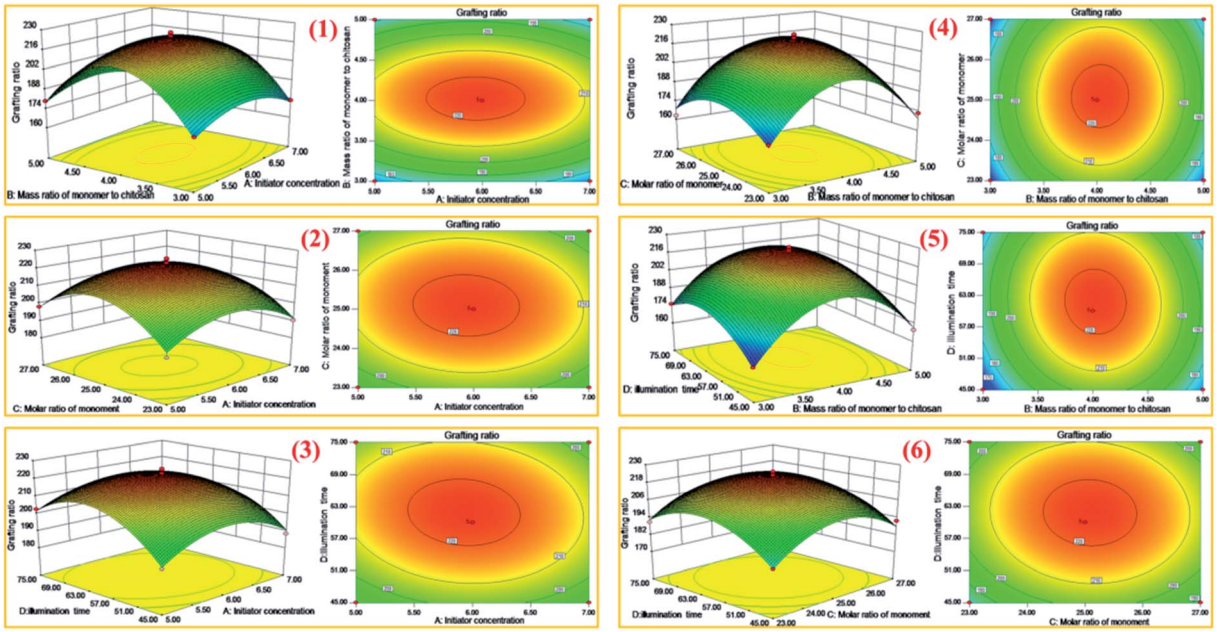

Fig. 4 Interaction of various factors on grafting ratio of poly(CTS-*g*-AM-MAPTAC). (1) Initiator concentration plus mass ratio of monomer to chitosan; (2) initiator concentration plus molar ratio of monomer; (3) initiator concentration plus illumination time; (4) mass ratio of monomer to chitosan plus molar ratio of monomer; (5) mass ratio of monomer to chitosan plus illumination time; (6) molar ratio of monomer plus illumination time.

conditions were optimized through a series of flocculation experiments. The results are shown in Fig. 5.

Fig. 5(1) shows the effect of pH on flocculation. The dosage of flocculants in the experiment were applied with the respective optimal dose under different pH conditions (S9 text†). As pH increased, the percent residual turbidity of the supernatants after flocculation all showed a "down-up" process. However, it can also be seen from the figure that the residual turbidity percentage of the supernatant varies little after poly(CTS-*g*-AM-MAPTAC) flocculation under different pH conditions, indicating that pH has less effect on this process. This phenomena can be explained by the change of zeta potential with pH. Therefore, pH = 4 was selected for all the subsequent experiments.

Fig. 5(2) shows the effect of poly(CTS-*g*-AM-MAPTAC) with different grafting rate on the effect of flocculation. With the increase of dosage, the percent residual turbidity of the supernatant after flocculation by poly(CTS-*g*-AM-MAPTAC) with different grafting rates all showed a "down-up" process. Furthermore, the three experiments all showed good turbidity removal effect at very low dose. In particular, the dosage of 3# flocculant was minimal and at that dosage the percentage residual percent turbidity of supernatant after flocculation was only 0.96%. As was previously mentioned, poly(CTS-*g*-AM-MAPTAC) has strong electrical neutralization under acidic conditions (pH = 4), and thus the 3# product with higher grafting rate exhibited more positive MAPTAC molecules and better treatment effect at lower dosage. However, after the dosage of flocculation exceeded 1.0 mg L^{-1}, the flocculation effect was significantly worse, that was, the phenomenon of "re-stability" when the flocculant dosage was excessive, and this deterioration phenomenon cannot be ignored. Therefore, in order to ensure a good flocculation effect and to avoid the occurrence of the glue particle "re-stability", the grafting rate of the flocculant should be controlled within the appropriate range. Compared with 3 #, the optimal dosage of 2 # product was not very different, and its "re-stability" phenomenon was not very obvious, so the better grafting product was determined to be 2 # product.

Fig. 5(3)a–d correspond to the flocculation process of PAMA, PAM, PAC and poly(CTS-*g*-AM-MAPTAC) on kaolin suspension. It can be seen that under the action of four flocculants, with the increase of dosage, the residual turbidity percentage of the supernatant also showed "down-up" process, and the corresponding zeta potential showed a gradual upward trend. The flocculation effect of poly(CTS-*g*-AM-MAPTAC) was significantly better than the other three flocculants. When the dosage of poly(CTS-*g*-AM-MAPTAC) was 0.4 mg L^{-1}, the residual turbidity of the supernatant was only 1.04%, which indicating a good application prospect. The excellent flocculation effect of poly(CTS-*g*-AM-MAPTAC) was mainly attributed to the synergistic reaction between the strong electrostatic attraction of the quaternary ammonium group and the strong bridging ability of long molecular chains to the colloidal particles. In addition, the large specific surface area and the loose porous fold structure of poly(CTS-*g*-AM-MAPTAC) also enhanced its ability to catch and sweep the flocculates in the late flocculation period, making the generated flocculation settle down quickly and improve the flocculation efficiency.[36–38]

Flocculation and sterilization of *E. coli* suspension. As with the kaolin flocculation removal experiment, this section also examined the effect of flocculant dosage, pH and grafting rate of poly(CTS-*g*-AM-MAPTAC) on the removal of *E. coli* in wastewater. The dosage of flocculants in the experiment were applied

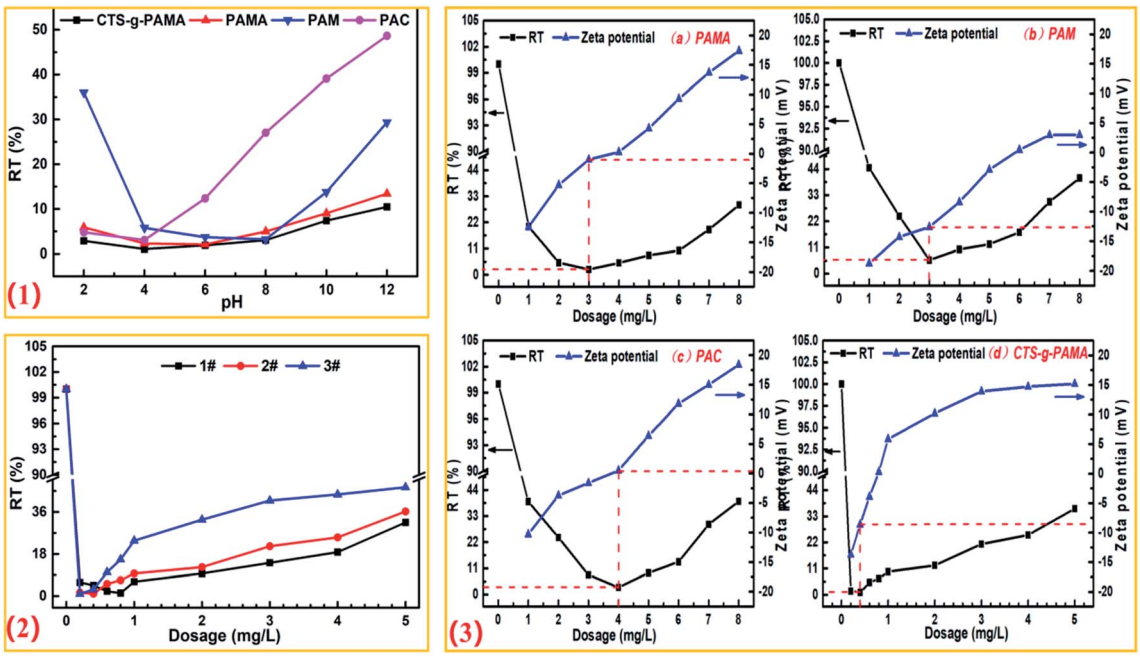

Fig. 5 Effect of experimental conditions on flocculation: (1) pH; (2) grafting rate; (3) locculant dosage.

with the respective optimal dose under different pH conditions (S10 text†). The experimental results are shown in Fig. 6.

RT% after flocculation with PAM or fungicide 1277 was greatly affected by pH, while, the treatment effect of PAMA and poly(CTS-*g*-AM-MAPTAC) was relatively stable, and poly(CTS-*g*-AM-MAPTAC) showed the best turbidity removal effect (Fig. 6-1a). As can be seen from the change of OD_{600} with pH in Fig. 6-1b, 1277 as a quaternary ammonium cationic active fungicide showed excellent bactericidal effect under acidic conditions, but rebounded as pH increased to alkaline. The bactericidal effect of small molecule microbicide 1277 was mainly the selective adsorption of bacteria by quaternary ammonium group, resulting in the bacterial surface was covered with high concentration of ions, and thus inhibiting or killing the bacteria.[39,40] It can be seen that poly(CTS-*g*-AM-MAPTAC) showed good bactericidal effect in the whole pH range, and was not affected by pH. In acidic conditions, quaternary ammonium groups in the grafted MAPTAC molecular chain played a bactericidal effect, this was similar to that of 1277. While in neutral/alkaline conditions, poly(CTS-*g*-AM-MAPTAC) as a polymer material formed a molecular film on the surface of bacteria, which hindered the material energy exchange inside and outside the cells and affected the normal metabolism of bacteria to play a role in inhibiting bacteria.

As shown in Fig. 6-2a, with the increase of the dosage, the RT% of the supernatant after the four flocculants treatment showed a downward trend, and the downward trend of poly(CTS-*g*-AM-MAPTAC) was particularly obvious. Subsequently, except for the flocculation "restabilization" phenomenon in the PAM experimental group, all the others slowly reached a stationary period, indicating other effects may be present in the flocculation mechanism of poly(CTS-*g*-AM-MAPTAC) on *E. coli* besides electroneutralization and adsorption bridging. When the dosage was less than 5 mg L^{-1}, the OD_{600} of 1277 and poly(CTS-*g*-AM-MAPTAC) supernatants showed a rapid decline stage, indicating that they all showed excellent bactericidal performance at low dosage. Although the dosage of 1277 was lower and the sterilization effect was more obvious, the flocculation effect was not ideal. However, poly(CTS-*g*-AM-MAPTAC) showed excellent treatment effect in flocculation and sterilization, comparatively.

According to Fig. S3-2,† the isoelectric points of *E. coli* suspension and poly(CTS-*g*-AM-MAPTAC) appeared at pH = 2.9 and pH = 8.2, respectively. The zeta potential of poly(CTS-*g*-AM-

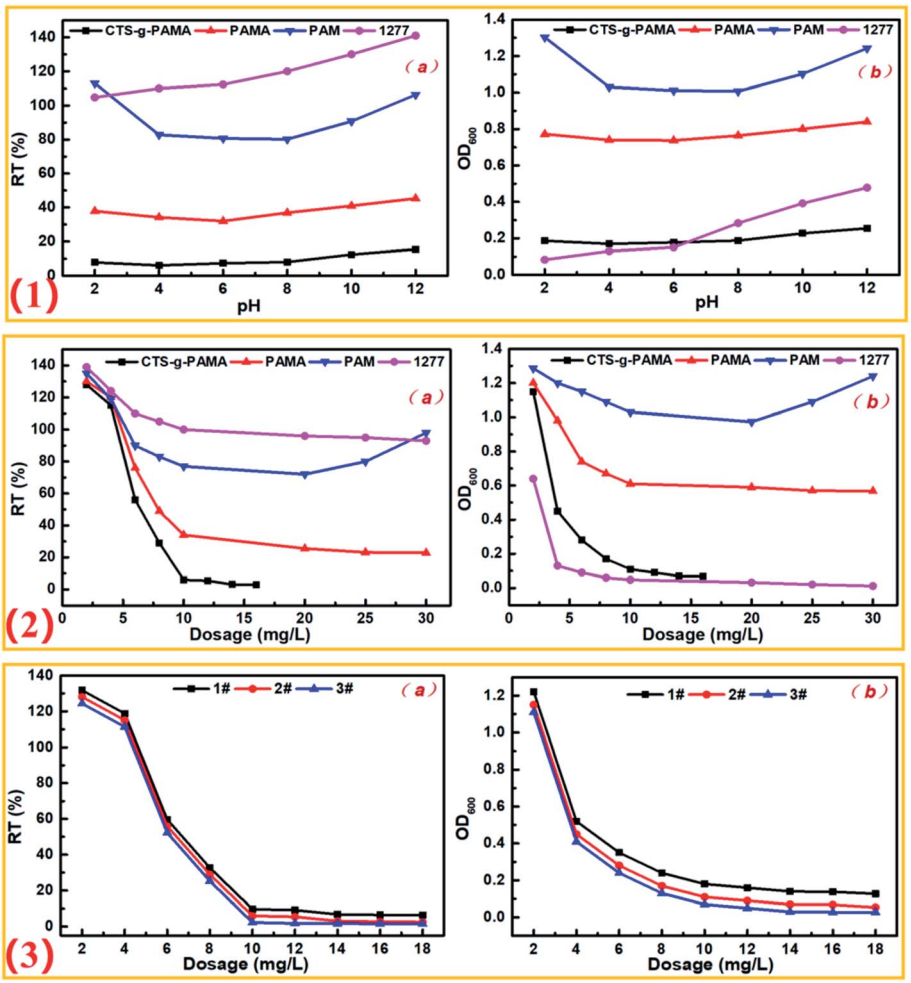

Fig. 6 Effect of experimental conditions on flocculation: (1) pH; (2) flocculant dosage; (3) grafting degree.

MAPTAC) was significantly higher than that of *E. coli* suspension. Therefore, it can be speculated that the electrical neutralization of poly(CTS-*g*-AM-MAPTAC) played an important role in the flocculation process. Therefore, 3# products with the highest grafting rate should theoretically have the best treatment effect, and this was also confirmed by the verification in Fig. 6-3. However, there are still some other pollutants (organic substances, colloidal particles, *etc.*) in the actual water body, which would still appear excessive "re-stability" similar to kaolin in the process of flocculation. Therefore, in order to avoid the deterioration of flocculation effect, 2# product with medium grafting rate was determined as the appropriate flocculant for *E. coli* suspension flocculation process.

Conclusion

In this paper, cationic monomers and polyacrylamide were grafted to the molecular chains of chitosan by UV light-induced polymerization. The cationic modification and the introduction of long-chain PAM molecules improved the dissolution properties of chitosan, but also the flocculation and bactericidal properties. In addition, the synthetic modified products had excellent acid and base resistance. All the instrumental characterization results confirmed the successful synthesis of poly(CTS-*g*-AM-MAPTAC). In order to promote the grafting rate of poly(CTS-*g*-AM-MAPTAC), Box–Behnken experiment design and respond surface method were employed to optimum the synthesis conditions. The optimum synthesis conditions were 6 moL L^{-1} for initiator concentration, 4 for mass ratio of total monomer to chitosan, 25% for monomer molar ratio, and 60 min for illumination time. The intrinsic viscosity and grafting rate of poly(CTS-*g*-AM-MAPTAC) prepared under the optimum condition were 5.4965 dL g^{-1} and 220.34%. Results of flocculation tests showed that the poly(CTS-*g*-AM-MAPTAC) 2# (202% of grafting rate, 5.12 of intrinsic viscosity) exhibited excellent flocculation and bactericidal performance.

Conflicts of interest

There are no conflicts to declare.

Acknowledgements

This research was supported by the National Natural Science Foundation of China (project no. 52000019), the China Postdoctoral Science Foundation (project no. 2021M693747), the Provincial and Ministerial Co-constructive of Collaborative Innovation Center for MSW Comprehensive Utilization (project no. shljzyh2021-21), the Chongqing Science and Technology Commission Project (project no. cstc2018jcyjAX0699), the Scientific and Technological Research Program of Chongqing Municipal Education Commission (project no. KJZD-M201900802, KJZD-K201800801), the Science and Technology Innovation Projects for College Students (project no. YKJCX2120607, 202211551023).

References

1 D. S. Kosyakov, N. V. Ul'yanovskii, M. S. Popov, T. B. Latkin and A. T. Lebedev, *J. Anal. Chem.*, 2018, **73**, 1260.
2 L. Ma and J. Liu, *Desalin. Water Treat.*, 2021, **231**, 297.
3 C. Abueva, H. S. Ryu, J. W. Min, P. S. Chung, H. S. You, M. S. Yang and S. H. Woo, *Int. J. Biol. Macromol.*, 2021, **182**, 1713.
4 V. Visconti, E. Coton, K. Rigalma and P. Dantigny, *Fungal Biol. Rev.*, 2021, **38**, 44.
5 S. Zhang, H. Zheng, X. Tang, C. Zhao, C. Zheng and B. Gao, *Chem. Eng. J.*, 2020, **382**, 122961.
6 X. Zheng, H. Zheng, Y. Zhou, Y. Sun, R. Zhao, Y. Liu and S. Zhang, *Colloids Surf., A*, 2019, **580**, 123746.
7 L. Feng, X. H. Li, W. C. Lu, Z. Liu, C. Xu, Y. Chen and H. L. Zheng, *Int. J. Biol. Macromol.*, 2020, **150**, 617.
8 W. Du, Y. Li, X. Xu, Y. Shang, B. Gao and Q. Yue, *J. Colloid Interface Sci.*, 2019, **533**, 692.
9 X. Li, H. Zheng, B. Gao, C. Zhao and Y. Sun, *Sep. Purif. Technol.*, 2017, **187**, 244.
10 X. Li, H. Zheng, B. Gao, Y. Sun, X. Tang and B. Xu, *RSC Adv.*, 2017, **7**, 208.
11 M. Pedersen, E. Vryonidis, A. Joensen and M. Tornqvist, *Food Chem. Toxicol.*, 2022, **161**, 112799.
12 M. Zhao, L. Deng, X. Lu, L. Fan, Y. Zhu and L. Zhao, *Environ. Sci. Pollut. Res.*, 2022, **29**, 41151.
13 L. Zhu, W. Jia, Q. Wang, P. Zhuang, X. Wan, Y. Ren and Y. Zhang, *Ecotoxicol. Environ. Saf.*, 2021, **224**, 112625.
14 S. M. Asharuddin, N. Othman, W. A. H. Altowayti, N. Abu Bakar and A. Hassan, *Environ. Technol. Innovation*, 2021, **23**, 101637.
15 A. Shemesh, Y. Zvulunov and A. Radian, *Sep. Purif. Technol.*, 2022, **278**, 119179.
16 Y. Sun, S. Zhou, W. Sun, S. Zhu and H. Zheng, *Sep. Purif. Technol.*, 2020, **241**, 116737.
17 E. I. Unuabonah, A. Adewuyi, M. O. Kolawole, M. O. Omorogie, O. C. Olatunde, S. O. Fayemi, C. Günter, C. P. Okoli, F. O. Agunbiade and A. Taubert, *Heliyon*, 2017, **3**, e00379.
18 R. P. Pandey, P. Kallem, P. A. Rasheed, K. A. Mahmoud, F. Banat, W. J. Lau and S. W. Hasan, *Chemosphere*, 2022, **289**, 133144.
19 X. Li, H. Zheng, B. Gao, Y. Sun, B. Liu and C. Zhao, *Chemosphere*, 2017, **167**, 71.
20 W. Sun, S. Zhou, Y. Sun and Y. Xu, *J. Environ. Sci.*, 2021, **99**, 239.
21 X. Xiao, Y. Sun, J. Liu and H. Zheng, *Sep. Purif. Technol.*, 2021, **267**, 118628.
22 H. E. Ali, S. M. Nasef and Y. H. Gad, *Carbohydr. Polym.*, 2022, **283**, 119149.
23 W. Deng, Y. Yan, P. Zhuang, X. Liu, K. Tian, W. Huang and C. Li, *Drug Delivery*, 2022, **29**, 399.
24 Y. Sun, Y. Yu, X. Zheng, A. Chen and H. Zheng, *Carbohydr. Polym.*, 2021, **261**, 117891.
25 L. Feng, X. Li, W. Lu, Z. Liu, C. Xu, Y. Chen and H. Zheng, *Int. J. Biol. Macromol.*, 2020, **150**, 617.

26 M. Gul, N. W. M. Zulkifli, M. A. Kalam, H. H. Masjuki, M. A. Mujtaba, S. Yousuf, M. N. Bashir, W. Ahmed, M. N. A. M. Yusoff, S. Noor, R. Ahmad and M. T. Hassan, *Energy Rep.*, 2021, **7**, 830.
27 A. Naeimi, A. Sharifi, A. R. Abhari, S. Farrokhzadeh and B. Jannat, *J. Mol. Struct.*, 2022, **1250**, 131696.
28 N. M. Daud, S. R. S. Abdullah and H. A. Hasan, *Process Saf. Environ. Prot.*, 2018, **113**, 184.
29 G. Sun, J. Zhang, W. Meng and L. Wang, *Water Supply*, 2020, **20**, 3625.
30 W. Zhang, W. Lv, X. Li and J. Yao, *Pigm. Resin Technol.*, 2020, **49**, 46.
31 R.-S. Kaarmukhilnilavan, A. Selvam, J. W. C. Wong and K. Murugesan, *Colloids Surf., A.*, 2020, **630**, 125177.
32 L. Ma, J. Liang, S. Wang, B. Yang, M. Chen and Y. Liu, *Environ. Technol.*, 2019, **40**, 44.
33 L.-W. Zhang, J.-R. Hua, W.-J. Zhu, L. Liu, X.-L. Du, R.-J. Meng and J.-M. Yao, *ACS Sustainable Chem. Eng.*, 2018, **6**, 1592.
34 J. Blockx, A. Verfaillie, O. Deschaume, C. Bartic, K. Muylaert and W. Thielemans, *Nanoscale Adv.*, 2021, **3**, 4133.
35 N. Chen, W. Liu, J. Huang and X. Qiu, *Int. J. Biol. Macromol.*, 2020, **146**, 9.
36 Y. Jeong, J.-I. Park, M. G. Ha, J.-S. Bae, Y. Choi, S.-A. Choi, Y.-K. Oh, H.-R. An, H. Kim, H. J. Kim, S. M. Lee, S. Lee, M. Lee, Y. C. Hong and H. U. Lee, *Ceram. Int.*, 2020, **46**, 23582.
37 F. Sun, H. Zhang, A. Qian, H. Yu, C. Xu, R. Pan and Y. Shi, *Sci. Total Environ.*, 2020, **720**, 137573.
38 W. Chen, J. Tang, P. Cheng, Y. Ai, Y. Xu and N. Ye, *Materials*, 2022, **15**, 925.
39 D. Bu, Y. Zhou, C. Yang, H. Feng, C. Cheng, M. Zhang, Z. Xu, L. Xiao, Y. Liu and Z. Jin, *Chin. Chem. Lett.*, 2021, **32**, 3509.
40 Q. Liu, J. Wang, C. Duan, T. Wang and Y. Zhou, *J. Hazard. Mater.*, 2022, **426**, 128074.